Journal of Catalysis 275 (2010) 140–148

Contents lists available at ScienceDirect

Journal of Catalysis

journal homepage: www.elsevier.com/locate/jcat

Facile preparation of supported noble metal nanoparticle catalysts with the aid of templating surfactants in mesostructured materials

Hu Wang, Jin-Gui Wang, Zhu-Rui Shen, Yu-Ping Liu, Da-Tong Ding, Tie-Hong Chen *

Institute of New Catalytic Materials Science, Key Laboratory of Advanced Energy Materials Chemistry (MOE), College of Chemistry, Nankai University, Tianjin 300071, PR China

ARTICLE INFO

Article history:
Received 12 May 2010
Revised 24 July 2010
Accepted 27 July 2010
Available online 30 August 2010

Keywords:
Quaternary ammonium surfactant
Hybrid mesostructured materials
Palladium
Allyl alcohol hydrogenation
Aerobic selective oxidation

ABSTRACT

Quaternary ammonium surfactants were generally used as templates in the synthesis of mesoporous materials, and the surfactants were removed by extraction or calcination to give the space of mesopores. Here with the cetyltrimethylammonium bromide templated mesostructured materials, we directly utilized the surfactants as capturing and stabilizing agents to prepare supported noble metal nanoparticle catalysts. The Pd-supported catalysts exhibited high and stable activity in hydrogenation of allyl alcohol (with a remarkably high turnover frequency of 5676 h^{-1}) and aerobic oxidation of benzyl alcohol. During the recycle use of the catalyst, though surfactants were gradually leached into the reaction medium, the amount of Pd in the catalyst remained constant within experimental error. It is facile and energy-saving to use directly the as-synthesized mesostructured materials as support for noble metal nanoparticles without further calcination or further modification treatment. This method is versatile to prepare other noble metal (such as Au and Pt) supported catalysts by altering the metal precursors.

1. Introduction

Mesoporous materials containing noble metal nanoparticles have attracted much attention owing to their potential application in catalysis [1–3]. Many strategies including impregnation [4,5], deposition–precipitation [6], in situ encapsulation [7–9], chemical vapor deposition (CVD) [10,11], and surface functionalization schemes [12–15] were reported to prepare supported metal nanoparticles on mesoporous materials. The impregnation method has been widely used because of its easy manipulation; however, it results in uncontrolled growth of metal particles with relatively large size. CVD is an efficient method for preparing nanoparticles or thin films, but the precursors are limited, and the devices are complicated. Au-supported MCM-41 was prepared by a modified deposition–precipitation method with the aid of ethylenediamine and surfactant-containing support, but a calcination procedure was followed to remove the occluded surfactant templates [16]. In the surface functionalization schemes, functional groups such as thiol or amino groups can be immobilized onto the inner walls of mesopores by grafting process with a silane coupling reagent. The grafted functional groups act as strong ligands to anchor the corresponding metal ions into the channels of mesoporous materials. However, due to some disadvantages, such as tedious synthesis and post-treatment procedures of the supports, employment of toxic and volatile organic solvents, energy-wasting in calcination and high costs of the reactants, large-scale applications of some reported method for preparing supported noble metal catalysts are still limited. Facile, mild and environmentally benign preparation method is still a challenge.

Cationic surfactants, such as cetyltrimethylammonium bromide (CTAB), have been prevalently used as templates for the synthesis of mesoporous materials. Generally, the templating surfactant micelles were removed by calcination or extraction to give the mesoporous voids for hosting other guest species. However, in the respect of metal nanoparticle supporting, removal of the surfactants would be less cost-efficient because alkylammonium ions have been proved to be good surface-stabilizing agents in the preparation and morphological control of noble metal nanoparticles [17–19].

Recently, as-synthesized MCM-41 was applied as basic catalyst in the Knoevenagel and Claisen–Schmidt condensation reactions. The catalyst showed higher catalytic activity than MCM-41 modified with Cs_2O or aminopropylsilyl group and exhibited long-term catalytic stability [20]. Kubota et al. used the as-synthesized MCM-41 catalyst for Knoevenagel condensation and Michael reaction with high catalytic activity and stability [21,22]. Although the channels of as-synthesized MCM-41 were filled with surfactants, the catalyst still exhibited high activity, and the excellent performance was ascribed to the basic $Si\text{-}O^-$ sites presented at the pore-mouth because the mesopores were occluded by the quaternary ammonium surfactants [20,23–25].

* Corresponding author. Fax: +86 22 23507975.
E-mail address: chenth@nankai.edu.cn (T.-H. Chen).

0021-9517/$ - see front matter © 2010 Elsevier Inc. All rights reserved.
doi:10.1016/j.jcat.2010.07.025

Here, we report a facile, novel and cost-effective approach to prepare supported noble metal nanoparticles with as-synthesized mesostructured materials by utilizing directly the templating surfactants as capturing and stabilizing agents. By the adsorption of noble metal precursors and reduction, the noble metal nanoparticles were confined and stabilized by the alkylammonium surfactants within the mesopores. Because the mesopores were occluded by the surfactants, the noble metal precursors would preferentially form complex with the surfactants near the opening of the mesopores, and after reduction the noble metal nanoparticles would be inclined to locate near the entrance of the mesopores. In hydrogenation of allyl alcohol and aerobic oxidation of benzyl alcohol, the as-prepared Pd-loaded catalysts exhibited enhanced activity and recycling stability.

2. Experimental

2.1. Preparation of Pd/as-synthesized MCM-41 catalysts

Preparation of as-synthesized MCM-41(as-M41): In a typical synthesis, CTAB (0.85 g) was dissolved in a mixture of water (200 g) and ammonium hydroxide (14.3 g, 30%). Tetraethoxysilane (4.37 g) was added to this homogeneous solution with vigorous stirring for 10 min and then heated at 80 °C for 2 h. The resultant solid was filtered off and then extensively washed with distilled water and then dried at 120 °C for 24 h. As-synthesized mesostructured amorphous titania (denoted as-T) and as-synthesized mesostructured titanium phosphate (denoted as-TP) were synthesized by quaternary ammonium surfactants as template according to the published procedure [26,27].

Preparation of Pd/as-M41: Typically, 1 g as-M41 was suspended in 25 mL aqueous H_2PdCl_4 solution of desired concentration and stirred at room temperature for 30 min. The resulted precipitate was filtered and washed with distilled water for several times. Without further drying procedure, the obtained light orange powder was reduced with a freshly prepared solution of $NaBH_4$ (0.1 M) at room temperature. The sample was filtered, washed extensively with distilled water, and dried at 60 °C to obtain black power (denoted as Pd/as-M41). We also prepared Au/as-M41 and Pt/as-M41 catalysts by the same method with $HAuCl_4$ and H_2PtCl_6 solution as the noble metal precursors, respectively.

2.2. Preparation of diamine-functionalized MCM-41 supported Pd catalyst

The as-M41 was calcined at 550 °C in air for 5 h to remove the surfactant. One gram of calcined MCM-41 was stirred vigorously in 50 mL dry toluene containing 1.0 mmol of N-[3-(trimethoxysilyl) propyl] ethylenediamine. This solution was heated to 110 °C for 10 h. The powder was collected by filtration, washed with 2-propanol and dried at 100 °C. The obtained functionalized MCM-41 was denoted as F-M41. Pd/F-M41 catalyst was prepared in a similar way of the Pd/as-M41 catalyst preparation.

2.3. Preparation of catalysts by methods of wetness impregnation and deposition–precipitation

For comparison, palladium was deposited on the MCM-41 by wetness impregnation method. For the 0.5%Pd/M41-imp catalyst, an aqueous solution of H_2PdCl_4 (4 mL, 0.012 mol/L) was added to the MCM-41 (1.0 g). The resulting powder was dried at 110 °C for 24 h and calcined in air at 500 °C for 6 h. The catalyst was denoted as Pd/M41-imp.

Gold was deposited on the calcined MCM-41 by homogenous deposition–precipitation method using urea as the precipitating agent. In a typical procedure, 0.3 g urea was dissolved in 30 mL of 1.73 mmol/L $HAuCl_4$ solution at the room temperature. MCM-41 support is then added to this solution. The temperature of the resulting slurry was increased gradually to 90 °C and maintained for 4 h. The solid was filtered, washed several times with distilled water, dried and then calcined at 300 °C for 4 h in static air. The catalyst was denoted as Au/M41-DP.

2.4. Catalytic reaction tests

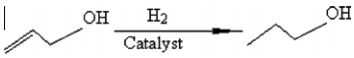

(1)

Catalytic hydrogenation of allyl alcohol (formula 1) was performed in a 50-mL, three-neck, round-bottomed flask at room temperature (30 ± 1 °C). H_2 was bubbled through a plastic pipe at the bottom of the solution at an invariable rate controlled by a valve. Suspended catalyst in 25 mL of ethanol was bubbled with H_2 for 30 min before adding 10 mmol allyl alcohol. In the recycled uses of the catalysts, 20 mmol allyl alcohol was used in the reaction.

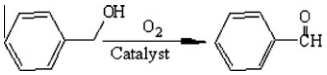

(2)

The liquid phase oxidation of benzyl alcohol (formula 2) was performed in a three-necked flask with a reflux condenser under magnetic stirring. The catalyst was added into the benzyl alcohol, and the mixture was heated by oil bath to reaction temperature, and O_2 flow (25 ml/min) was bubbled into the liquid.

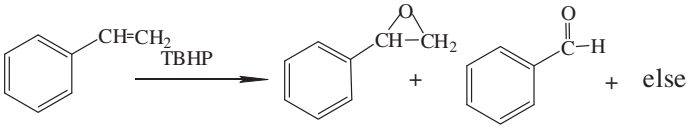

(3)

The selective oxidation of styrene (formula 3) was performed in a three-necked flask with a reflux condenser under magnetic stir. The Au-supported catalyst (100 mg) was added to the toluene (10 mL) solution containing 40 mg of styrene and 200 mg TBHP (*tert*-butyl hydroperoxide). Dodecane (30 mg) was added as internal standard substance. The mixture was heated by oil bath to 80 °C.

After the reactions, the catalyst was separated by centrifugation, and the liquid products were analyzed by a gas chromatograph (GC-7800) with a flame ionization detector, using a FFAP column and N_2 as carrier gas.

2.5. Characterization methods

The Pd (or Au) content was determined by inductively coupled plasma (ICP) optical emission spectrometry using a Thermo Jarrell-Ash ICP-9000(N + M). Powder X-ray diffraction (XRD) patterns were recorded on a Bruker D8 Focus with Cu Kα radiation (40 kV, 40 mA). Transmission electron microscopy (TEM) and energy-dispersive X-ray spectroscopy (EDX) measurements were taken using a Philips Tecnai F20 microscope. All samples subjected to TEM measurements were ultrasonically dispersed in the ethanol and dropped on copper grids. X-ray photoelectron spectroscopy (XPS) measurements were taken with a Kratos Axis Ultra DLD spectrometer employing a monochromated Al Kα X-ray source ($h\nu$ = 1486.6 eV). Thermogravimetry (TG) was performed with a Rigaku thermogravimetry–differential thermal analysis analyzer in air with the heating rate of 20 K/min.

3. Results and discussion

3.1. Preparation of Pd/as-M41 samples

As shown in Scheme 1, at room temperature the surfactants in the channels of as-M41 adsorbed $PdCl_4^{2-}$ ions specifically and quickly from the aqueous solution of H_2PdCl_4. After reduction by $NaBH_4$ solution at room temperature, well-dispersed Pd nanoparticles were formed and hosted by the as-M41. During the preparation process, when the as-M41 was added into H_2PdCl_4 solution under stirring, within several minutes the color of as-M41 changed from white to light orange (Fig. 1). After filtration, the filtrate became transparent and colorless. For the case of 1.0% Pd loading, ICP analysis indicated that the concentrations of Pd in the starting solution and in the filtrate were 380 ppm and 2.7 ppm, respectively, indicating that over 99% of the total $PdCl_4^{2-}$ ions were adsorbed in as-M41. The coordination between the quaternary ammonium cations and $PdCl_4^{2-}$ anions would be responsible for the rapid adsorption of $PdCl_4^{2-}$. When the calcined MCM-41 was used in the above procedure, it did not adsorb $PdCl_4^{2-}$ and the color of the solution and the powder did not change.

It is conceivable that the $PdCl_4^{2-}$ ions would coordinate mainly with the CTA^+ groups located at the opening of the meso-channels (pore-mouth). The penetration of the $PdCl_4^{2-}$ ions deep inside the pore would be less favorable because the mesopores were occluded with surfactants, and there were enough CTA^+ groups present near the entrance of pore to host the $PdCl_4^{2-}$ ions. Therefore, the Pd nanoparticles formed after reduction would locate near the pore-mouth of the mesopores. Furthermore, the Pd nanoparticles were confined and stabilized by the surfactant micelles in the mesopores, and thus the size of the nanoparticles would be small. The loading of palladium in the catalyst after reduction was 1.09% based on ICP measurement, and this value was in good agreement with the designed loading of 1.0% in the $PdCl_4^{2-}$ adsorption process.

Without calcination, modification or using organic solvent, the preparation method reported here is facile and energy-saving. This method is versatile to prepare other supported nanosized noble metal catalysts by altering the metal precursors, such as Au/as-M41 and Pt/as-M41. Meanwhile, other mesostructured materials, such as titania and titanium phosphate, were synthesized templated by quaternary ammonium surfactants to support noble metal nanoparticles by the same scheme.

3.2. Characterization of Pd/as-M41 samples

As shown in Fig. 2, the low-angle XRD patterns of as-M41, 1%Pd/as-M41 before reduction and 1%Pd/as-M41 after reduction displayed three diffraction peaks of 2D hexagonal mesostructure, respectively. The wide-angle XRD pattern of 1%Pd/as-M41 (Fig. 3a) did not display diffraction peaks of Pd, implying that the size of Pd nanoparticles could be too small to be detected by XRD. If the Pd/as-M41 was calcined at 500 °C for 2 h, PdO particles in relatively larger size were formed and gave rise to the diffraction peaks in the XRD pattern (Fig. 3b).

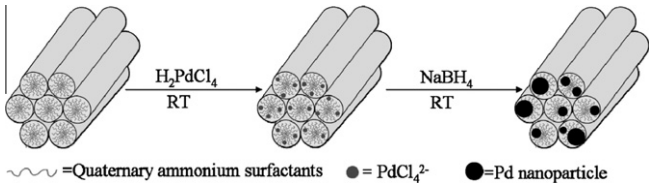

Scheme 1. Illustration of the preparation of Pd/as-M41 catalyst. RT means room temperature.

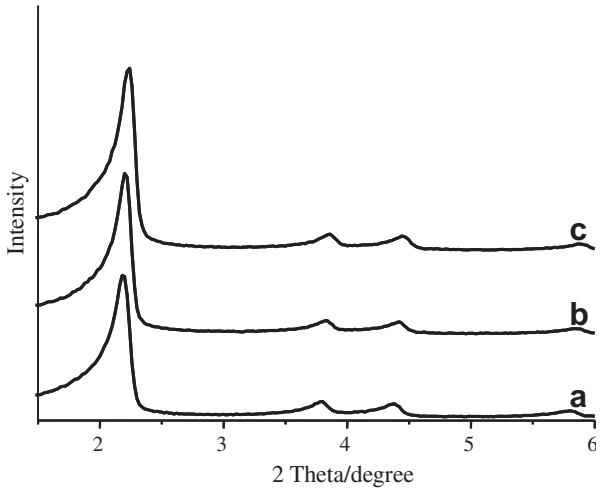

Fig. 2. Low-angle XRD patterns of (a) as-M41, (b) Pd/as-M41 before reduction, (c) Pd/as-M41 after reduction.

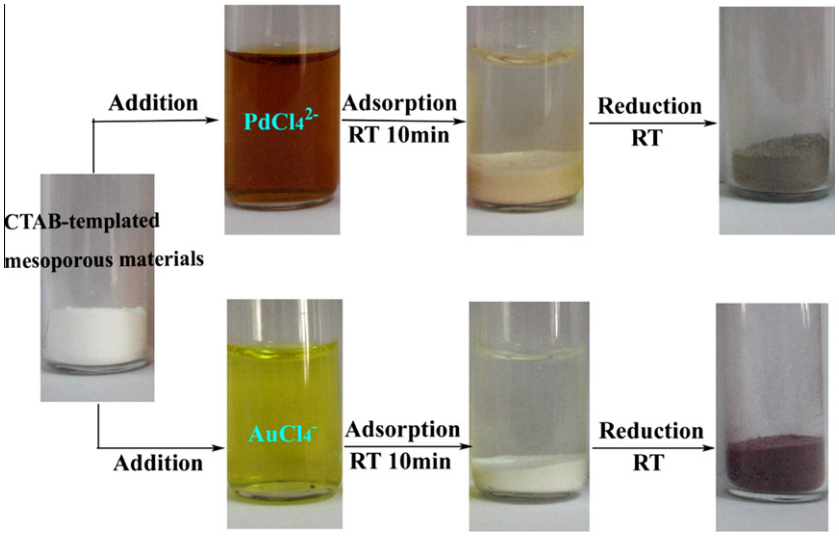

Fig. 1. Photographs of preparation procedure of CTAB-templated mesostructured materials supported noble metal nanoparticle catalysts.

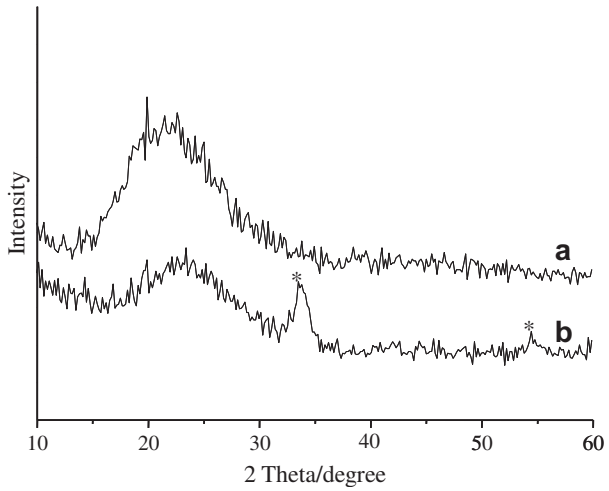

Fig. 3. Wide-angle XRD patterns of (a) Pd/as-M41 and (b) Pd/as-M41 after calcination at 500 °C. The asterisks indicate the diffraction peaks of PdO.

The dispersion of the Pd nanoparticles in Pd/as-M41 catalyst was analyzed by TEM analysis. As shown in Fig. 4, at low magnification (Fig. 4a and b) there were hardly any visible Pd nanoparticles, indicating that the Pd nanoparticles could be small, in agreement with the result of the XRD pattern. The small size of the Pd nanoparticles would result in low contrast in the TEM images so they could not be clearly distinguished from the surfactant/silica matrix. Similar phenomenon was also reported by Lu et al. for supported Pd clusters in mesoporous carbon, and due to the small particle size no visible Pd clusters could be found in the carbon framework by TEM analysis [28]. In the TEM images with higher magnification, occasionally only a few Pd nanoparticles could be identified which were located inside the mesopores (Fig. 4c and d, indicated by arrows). The dispersion of palladium clusters inside the as-M41 could be proved by EDX analysis. As shown in Fig. 5 and Fig. S1 (in Supporting Information), though there were no observable Pd nanoparticles in TEM images, Pd signal could be well detected in the EDX spectra collected from different local areas. To further prove the presence of Pd clusters in the catalyst, the Pd/as-M41 was calcined and TEM revealed that many Pd (actually PdO) nanoparticles appeared on the external surface of the MCM-41 particles (Fig. 6), due to the aggregation and outtransfer of the dispersed Pd clusters during burn of the surfactants. In this case, the diffraction peaks of PdO appeared in the wide-angle XRD pattern (Fig. 3b). According to above results, in the Pd/as-M41 catalyst the size of the Pd nanoparticles (or clusters) was small and well dispersed.

The confinement effect of the mesopores on Pd nanoparticles during the reduction of the surfactant-hosted $PdCl_4^{2-}$ could be proved by a control experiment. $PdCl_4^{2-}$/CTAB solution was prepared, and after $NaBH_4$ reduction a homogenous black solution was obtained. The Pd particles were then observed by TEM, and

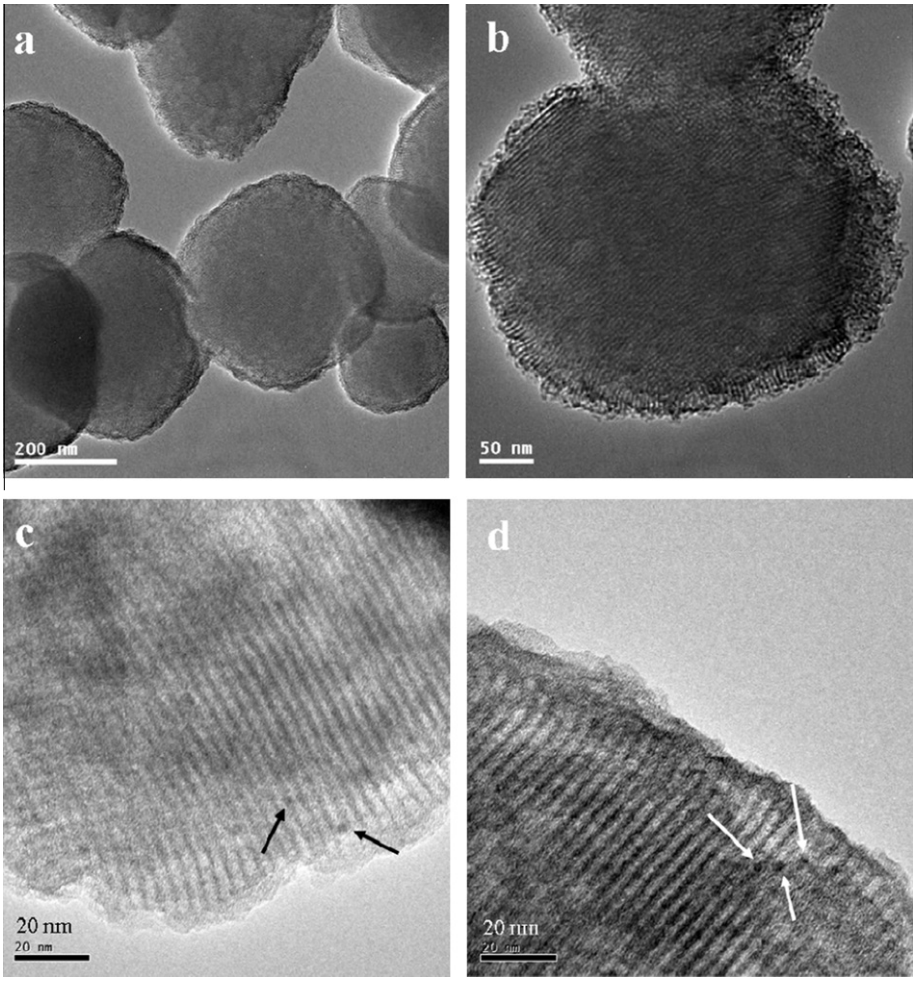

Fig. 4. TEM image of 1.0%Pd/as-M41, the arrows indicate a few observable Pd nanoparticles.

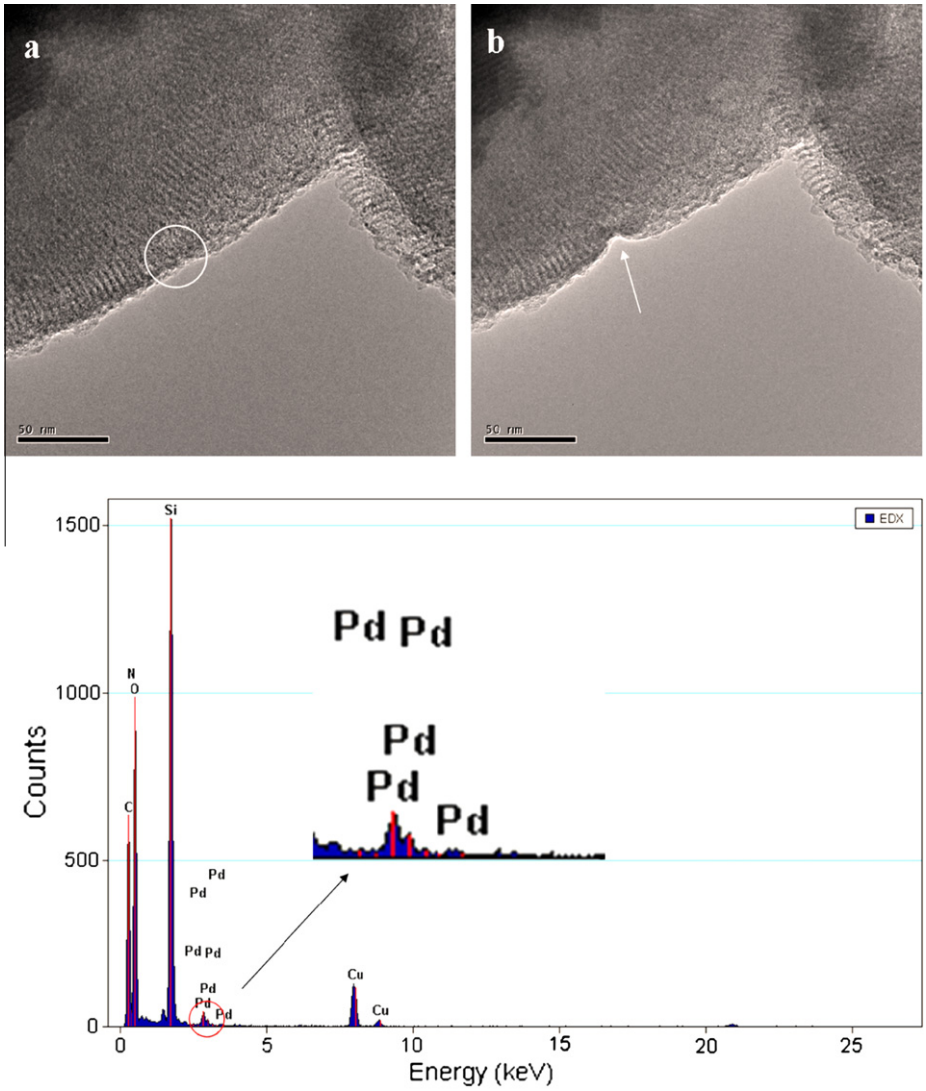

Fig. 5. TEM images and EDX spectrum (collected from the circle area) of the 1.0% Pd/as-M41 catalyst. The arrow in (b) indicates the area deformed by the irradiation of the electron beam after EDX measurement.

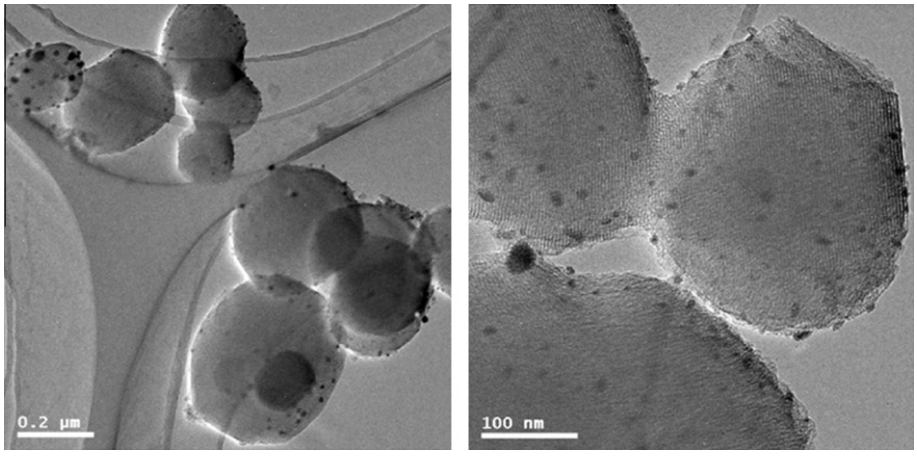

Fig. 6. TEM images of Pd/as-M41catalyst after calcination.

the average particle size was about 8 nm (Fig. S2, Supporting Information), which was much larger than that of the Pd nanoparticles located within the as-M41.

Before reduction of the sample, the XPS spectrum of Pd 3d (Fig. 7a) displayed two peaks at 342.3 eV (Pd $3d_{3/2}$) and 336.9 eV (Pd $3d_{5/2}$), which were ascribed to Pd^{2+}. Fig. 7b shows the Pd 3d

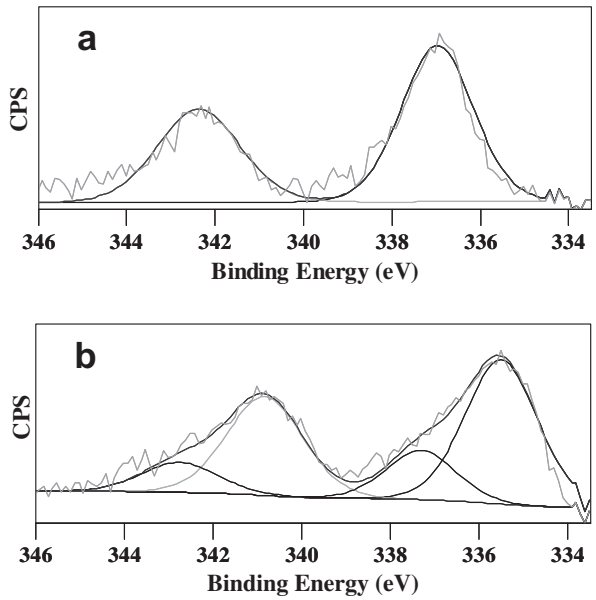

Fig. 7. Pd 3d XPS spectra of 1.0%Pd/as-M41: (a) before $NaBH_4$ reduction and (b) after reduction.

XPS spectrum of Pd/as-M41, and the peaks at 340.8 eV (Pd $3d_{3/2}$) and 335.5 eV (Pd $3d_{5/2}$) were ascribed to Pd^0 in the catalyst. The shoulders at 342.7 eV (Pd $3d_{3/2}$) and 337.3 eV (Pd $3d_{5/2}$) were due to surface oxidation of the palladium nanoparticles upon exposure in air. Fig. S3a (Supporting Information) shows the XPS spectrum of Cl 2p of Pd/as-M41 before reduction, in which obvious Cl 2p signal was observed. The formation of $[CTA^+]_2[PdCl_4^{2-}]$ complex has been verified by other literature [17,29]. In the XPS spectrum of Pd/as-M41, no Cl could be detected (Fig. S3b), indicating that the Cl^- anions were washed out of the catalyst after reduction.

3.3. Catalytic experiments

Using 0.5%Pd/as-M41 catalyst as a representative, catalytic activity was tested by a model hydrogenation reaction of allyl alcohol to 1-propyl alcohol, and the results were listed in Table 1. A blank experiment carried out without catalyst showed no conversion, even after 12 h of hydrogen treatment. The 0.5%Pd/as-M41 catalyst gave a remarkably high turnover frequency (TOF) (up to 5676 h^{-1}) with the 100% conversion for 45 min. For the 0.5 wt%Pd/MCM4-imp prepared by impregnation method, the conversion was only 80% for 45 min. For comparison, the TOF was 2944 h^{-1} for the Pd/diamine-functionalized mesopolymer working under the same reaction condition [30]. The reaction speed was relatively slow with Pt/as-M41 as catalyst, and after 45 min of reaction, the conversion was only 15% but with 100% selectivity toward 1-propyl alcohol. After 540 min of reaction, the conversion reached 100% with an excellent selectivity of 99% and a good TOF of 867 h^{-1}.

In general, surface functionalization is a prevalent strategy for the preparation of supported Pd/MCM-41 catalyst [31]. The internal surface of MCM-41 was generally modified by grafting silane coupling agents. For comparison, diamine-functionalized MCM-41 supported Pd catalyst (0.5%Pd/F-M41) was prepared and used in the hydrogenation reaction of allyl alcohol. After 45 min of reaction, the conversion was only 64%. It took longer time (70 min) than that for 0.5%Pd/as-M41 (45 min) when the conversion reached 100%. The lower activity of the 0.5%Pd/F-M41 sample could be attributed to the longer diffusion path for the reactants to reach the active sites, which located deeper inside the mesopores. Because hydrogen was involved in the liquid reaction system, the gas phase would be difficult to diffuse into the meso-channel. In contrast, the high activity of 0.5%Pd/as-M41 catalyst in the hydrogenation reaction of allyl alcohol could be attributed to the active sites presented near the pore-mouth.

Aerobic oxidation of alcohols has been intensively studied in recent years due to its economic and environmental advantages, and different noble metal supported catalysts were tested on this reaction [32]. Kaneda and coworkers [33,34] reported that phenylethanol and benzyl alcohol could be oxidized by hydroxyapatite supported Pd nanoparticles with high turnover frequencies. Hutchings and coworkers [35,36] showed that TiO_2-supported Au–Pd alloy nanocrystals give significantly enhanced activity for alcohol oxidation compared with monometallic Au or Pd catalysts. Prati and coworkers [37,38] also investigated alloy effect of Au–Pd and Au–Pt catalysts in alcohol oxidation. Corma and coworkers have shown that gold nanoparticles transform nanocrystalline cerium oxide from a stoichiometric oxidant into a catalytic material for the oxidation of alcohols with high TOFs and selectivities [39–41]. Here, the catalytic activities of the Pd/as-M41 catalysts were measured by aerobic oxidation of benzyl alcohol, and the results were listed in Table 2. The main product was benzaldehyde; however, further oxidation of benzaldehyde could occur to give benzoic acid, and benzylbenzoate was produced by esterification of benzoic acid and benzyl alcohol. The catalysts exhibited good activities under base- and solvent-free condition. The 0.5%Pd/as-M41 gave a high TOF (>1000 h^{-1}). Comparison with the results between Entry 1, 7, and 8, the 0.5%Pd/F-M41 and 0.5%Pd/M41-imp catalysts presented lower activity than that of the 0.5%Pd/as-M41 sample in oxidation of benzyl alcohol.

In the Knoevenagel and Claisen–Schmidt condensation reactions, the as-synthesized MCM-41 catalyst exhibited higher catalytic activity than that of the calcined MCM-41 modified with

Table 1
Performance of the catalysts in the hydrogenation of allyl alcohol.[a]

Entry	Catalyst	Time (min)	Conv. (%)	Selec.[b] (%)	TOF[c] (h^{-1})
1	0.5%Pd/as-M41	45	100	78	5676
2	1.0%Pd/as-M41	30	100	80	4257
3	0.5%Pt/as-M41	540	100	99	867
4	0.5%Pd/as-TP	45	100	75	5676
6	0.5%Pd/as-T	45	100	78	5676
7	0.5%Pd/F-M41	45	64	74	3632
8	0.5%Pd/M41-imp	45	80	80	4541

[a] H_2 flow, 40 mL min^{-1}; 30 °C; 25 mL ethanol as solvent; catalyst, 0.05 g; allyl alcohol, 10 mmol.
[b] The by-product was acetone.
[c] The TOF was calculated by the moles of substrates converted per mole of Pd per hour.

Table 2
Performance of the catalysts in the aerobic oxidation of benzyl alcohol.[a]

Entry	Catalyst	Time (h)	Conv. (%)	Selec.[b] (%)	TOF[c] (h^{-1})
1	0.5%Pd/as-M41	6	79	92	1359
2	1.0%Pd/as-M41	5	84	90	867
3	0.5%Pd/as-TP	6	78	92	1341
4[d]	1.0%Au/as-TP	6	40	91	637
5	0.5%Pd/as-T	6	77	90	1325
6[d]	1.0%Au/as-T	6	63	60	1003
7	0.5%Pd/F-M41	6	31	87	533
8	0.5%Pd/M41-imp	6	16	92	275

[a] O_2 flow, 25 mL min^{-1}; 100 °C; solvent-free reactions; catalyst, 0.1 g; benzyl alcohol, 48.5 mmol.
[b] The by-products were benzoic acid and benzylbenzoate.
[c] The TOF was calculated by the moles of substrates converted per mole of Pd per hour.
[d] The Entry 4, 6, K_2CO_3, 0.1 g.

Cs_2O or aminopropylsilyl group. Because the basic sites present inside the channels were inaccessible for the reactants, the high activity was attributed to the active sites present at the pore-mouth [20]. In our case, considering the different catalytic performance in the two model reactions between 0.5%Pd/as-M41 and 0.5%Pd/F-M41 catalysts, the latter suffered from the disadvantage of prolonged reaction time and lower activity. This result might be due to different location of Pd nanoparticles in the two catalysts. The active sites near the pore-mouth would exhibit better performance than those located in the interior of the mesopores. The resistance of mass transport was eliminated when the reaction took place at pore-mouth. Therefore, the reactant (benzyl alcohol or allyl alcohol) could be easy to reach the Pd active sites. In addition, when gas phase was involved in the liquid reaction system, the gas was difficult to diffuse into the meso-channels, and this is another factor resulting in lower catalytic performance of amino-functionalized M41 supported Pd catalyst.

Supported gold catalysts are promising in many reactions such as aerobic oxidation of alcohol [39–41], selective oxidation of styrene [42,43], and propylene epoxidation with O_2 and H_2 [44–46]. Here, the catalytic performance of 0.25% Au/as-M41 was tested by selective oxidation of styrene in toluene at 80 °C with anhydrous TBHP as oxidant, and the results were listed in Table 3. The catalytic data of Au/as-M41, Au/as-T, and Au/as-TP were more or less the same, representing the catalytic behavior of the surfactant-hosted gold nanoparticles. The conversion of styrene was similar to that by Au_{25} clusters on hydroxyapatite at the same reaction condition [42]. However, the selectivities of products were close to the result of thiolate-protected Au nanoclusters catalyst with O_2 as the oxidant [43]. The catalyst prepared by deposition–precipitation method (0.25%Au/M41-DP) was also tested, and it exhibited lower conversion than that of 0.25%Au/as-M41.

3.4. Stability tests of the catalysts

In order to verify the catalytic stability of Pd/as-M41, the catalyst was repeatedly used in the hydrogenation of allyl alcohol and aerobic oxidation of benzyl alcohol, respectively. In hydrogenation of allyl alcohol, the substrate was doubled so that the conversion was less than 100%, and by this way the effect of the recycled catalysts could be compared. After one run of catalytic reaction, the catalyst was separated from the reaction mixture by centrifugation, thoroughly washed with ethanol, and then reused as catalyst for next run under the same condition. As shown in Table 4, the catalyst remained similar activity and selectivity after eight runs, indicating the reusability and stability of the catalyst in hydrogenation reaction of allyl alcohol. For the 0.5%Pd/as-M41 catalyst, the conversion was 67% after 45 min, and the TOF became as high as 7606 h^{-1}.

In the recycling experiments of aerobic oxidation of benzyl alcohol, 0.5%Pd/as-M41 catalyst exhibited high stability and reusability. After recycling use of the catalyst for eight times, the benzyl alcohol conversion and benzaldehyde selectivity were essentially constant within experimental error (Table 3). When the CTAB-templated titania was used as the substrate (0.5%Pd/as-T), benzyl alcohol conversion and benzaldehyde selectivity were essentially constant within experimental error (Table S1 in Supporting Information).

Table 3
Performance of the Au catalysts in selective oxidation of styrene with TBHP as oxidant.[a]

Catalysts	Conv. (%)	Selec. (%)		
		Styrene epoxide	Benzaldehyde	Else[b]
0.25%Au/as-M41	93	22	73	5
0.25%Au/T	90	25	68	7
0.25%Au/TP	89	28	66	6
0.25%Au/M41-DP	70	7	88	5

[a] TBHP, 200 mg; 80 °C; 10 mL toluene as solvent; catalyst, 0.1 g; styrene, 40 mg; reaction time, 10 h.
[b] Else products include benzoic acid and acetophenone.

Table 4
Recycling performance of the 0.5%Pd/as-M41[a] catalyst in allyl alcohol hydrogenation and solvent-free aerobic oxidation of benzyl alcohol.

Catalytic cycle	Hydrogenation of allyl alcohol[b]		Oxidation of benzyl alcohol[c]	
	Conv. (%)	Selec. (%)	Conv. (%)	Selec. (%)
1	67	78	78	92
2	65	77	76	93
3	68	75	80	90
4	67	79	79	92
5	65	75	79	92
6	62	78	77	93
7	64	76	80	90
8	66	77	78	91

[a] The loading of Pd in the catalyst was 0.54% by ICP analysis.
[b] Reaction condition: H_2 flow, 40 mL min^{-1}; 30 °C; 25 mL ethanol as solvent; catalyst, 0.05 g; allyl alcohol, 20 mmol; time, 45 min.
[c] Reaction condition: O_2 flow, 25 mL min^{-1}; 100 °C; solvent-free reactions; catalyst, 0.1 g; benzyl alcohol, 48.5 mmol; time, 6 h.

The Pd/as-M41 catalyst was an inorganic–organic hybrid mesostructured material, and the possible leaching of CTA^+ surfactants and Pd nanoparticles during the reactions must be investigated, even though the catalyst exhibited stable activity in repeated uses. As reported by other groups, who used as-synthesized MCM-41 as catalyst in the Michael addition and Knoevenagel condensation reaction [21,25], partial leaching of the surfactants was observed in the reaction process. Kubota et al. [21] used as-synthesized MCM-41 in Michael addition reaction at 30 or 80 °C with benzene as solvent, and the weight loss after third run was less than 2% or 5% of the initial weight, respectively. According to Cardoso and coworkers, when as-synthesized MCM-41 was used in the Knoevenagel condensation reaction at 50 °C in the presence of toluene as solvent, the loss of mass was 53.5% in the recovered catalyst after the fourth use, while the value for the fresh catalyst was 54.2% [25]. Here to gain better insight into the stability of Pd/as-M41 catalyst, TG and ICP analyses were used to determine the weight loss and palladium content in the fresh and reused catalysts. Though the 0.5%Pd/as-M41 catalyst exhibited good activity in allyl alcohol hydrogenation and benzyl alcohol selective oxidation reactions, in order to enhance the veracity of the analysis results, 1.0%Pd/as-M41 sample was selected on purpose in the quantitative analysis. The stable performance after 8 runs of recycling tests for the 1.0%Pd/as-M41 catalyst was displayed in Table S2 in Supporting Information.

As shown in Table 5, the weight loss of the fresh 1.0%Pd/as-M41 catalyst was 35.8%, which was assigned to the decomposition of CTA^+ surfactants. The loading of palladium was 1.09% for the fresh catalyst by ICP measurement (Table 5, Entry 1). In the reaction of allyl alcohol hydrogenation, the weight loss of the reused catalyst became 30.7% and 27.3% after recycling uses for 4 and 8 times, respectively. For aerobic oxidation of benzyl alcohol, the weight loss of the reused catalyst was 33.3%, 22.2%, and 21.4% after recycling uses for 1, 4, and 8 times, respectively. The continuous weight loss of the catalysts indicated gradual leaching of the surfactants during the reactions. However, the amount of palladium in the recovered catalyst became 1.18% and 1.22% after 4 and 8 runs in hydrogenation, and 1.12%, 1.34%, and 1.37% after 1, 4, and 8 runs in oxidation, respectively. It is not surprising to see the increasing Pd content in the reused catalysts, due to the gradual leaching of

Table 5
Weight loss by TG and Pd content of 1.0%Pd/as-M41 catalysts before and after reaction.

Entry	Catalyst	Loss of mass (%)[a]	Pd (%)[b]	Pd(%)-SiO_2[c]
1	1.0%Pd/as-M41	35.8	1.09	1.70
2	1.0%Pd/as-M41-H-4[d]	30.7	1.18	1.70
3	1.0%Pd/as-M41-H-8	27.3	1.22	1.68
4	1.0%Pd/as-M41-O-1[e]	33.3	1.12	1.68
5	1.0%Pd/as-M41-O-4	22.2	1.34	1.72
6	1.0%Pd/as-M41-O-8	21.4	1.37	1.74

[a] Weight loss from TG curve between 150–600 °C.
[b] Pd weight percent in the catalyst detected by ICP measurement.
[c] Calculated Pd weight percent in the catalyst by deduction of the weight loss of the organic species. The oxidation of Pd and dehydroxylation of the silica during the TG measurements were not taken into account.
[d] H-*n*: the catalyst was reused in hydrogenation of allyl alcohol for *n* times.
[e] O-*n*: the catalyst was reused in aerobic oxidation of benzyl alcohol for *n* times.

the surfactants. For easy comparison, the Pd content was calibrated by deduction of the weight loss of the organic species, and the calculated Pd content values were listed in Table 5. It could be clearly found that the Pd content in the reused catalysts remained unchanged within experimental error, indicating that there was almost no Pd leaching in the reaction system even after repeated uses. This point was in good agreement with the experiment, i.e., when extra allyl alcohol (10 mmol) was added into the filtrate after extraction of the catalyst, no further conversion occurred after 45 min at the same reaction condition as was detected by GC. This indicated that no observable leaching of the Pd nanoparticles into the solution during the reaction.

As discussed above, in the Pd/as-M41 the Pd nanoparticles were stabilized by the CTA^+ surfactants. The gradual loss of the surfactants during the catalytic reactions would probably result in the partial leaching of the Pd nanoparticles; however, the Pd content in the catalyst remained unchanged. To explain this point, the black solution of CTAB-stabilized Pd nanoparticles was prepared as described previously. When proper amount of as-M41 (corresponding to 1 wt% Pd loading) was added in the solution, it was found that the CTAB-stabilized Pd nanoparticles were adsorbed by as-M41, and the black solution became colorless (Fig. S4 in Supporting Information). This implies though some Pd nanoparticles could be leached together with the surfactants from the Pd/as-M41 during the catalytic reactions, those disassociated surfactant-stabilized Pd nanoparticles in the reaction solvent could be adsorbed back by the catalyst, while the extracted surfactants were irreversibly lost. This could explain why the loss of the surfactants would not influence the stability of the Pd nanoparticles in the catalyst.

4. Conclusions

In summary, a facile method was presented to prepare supported noble metal catalysts by using as-synthesized mesostructured materials as the host. Other than the role of templating for mesopores, the surfactants played a new role of capturing and stabilizing agents to prepare supported noble metal nanoparticles. The specific interaction between the alkylammonium surfactants and $PdCl_4^{2-}$ at room temperature offered an easy control of Pd loadings. The Pd/as-M41 catalyst exhibited higher catalytic activity in hydrogenation of allyl alcohol and aerobic oxidation of benzyl alcohol reactions than that of the amino-functionalized MCM-41 supported Pd catalyst. Partial leaching of surfactants was observed in the recycling uses of the catalyst. However, the catalyst still showed high activity because no obvious leaching of Pd was observed in the process. The result was confirmed by the recycling uses of the catalyst, which exhibited stable catalytic activity in eight consecutive reactions for two model reactions. The as-synthesized mesostructured materials have a great advantage as the support of the noble metal nanoparticles, because they can be used as support directly, without further calcination or modification. Due to the facile preparation process and high catalytic performance, the hybrid catalysts would be promising in practical applications at relative low temperature.

Acknowledgments

This work was supported by NSFC (20873070, 20973095), National Basic Research Program of China (2009CB623502), RFDP (200800550007), NCET of Ministry of Education (NCET-07-0448) and MOE (IRT-0927).

Appendix A. Supplementary material

Supplementary data associated with this article can be found, in the online version, at doi:10.1016/j.jcat.2010.07.025.

References

[1] J.M. Campelo, D. Luna, R. Luque, J.M. Marinas, A.A. Romero, ChemSusChem 2 (2009) 18.
[2] R.J. White, R. Luque, V.L. Budarin, J.H. Clark, D.J. Macquarrie, Chem. Soc. Rev. 38 (2009) 481.
[3] A. Taguchi, F. Schueth, Micropor. Mesopor. Mater. 77 (2005) 1.
[4] X. Chen, H.Y. Zhu, J.C. Zhao, Z.F. Zheng, X.P. Gao, Angew. Chem. Int. Ed. 47 (2008) 5353.
[5] A. Fukuoka, H. Araki, J. Kimura, Y. Sakamoto, T. Higuchi, N. Sugimoto, S. Inagaki, M. Ichikawa, J. Mater. Chem. 14 (2004) 752.
[6] P. Haider, A. Baiker, J. Catal. 248 (2007) 175.
[7] U. Junges, W. Jacobs, I. Voigt-Martin, B. Krutzschc, F. Schueth, J. Chem. Soc. Chem. Commun. (1995) 2283.
[8] P. Krawiec, E. Kockrick, P. Simon, G. Auffermann, S. Kaskel, Chem. Mater. 18 (2006) 2663.
[9] A.K. Prashar, R.P. Hodgkins, R. Kumar, R.N. Devi, J. Mater. Chem. 18 (2008) 1765.
[10] P. Serp, P. Kalck, R. Feurer, Chem. Rev. 102 (2002) 3085.
[11] T. Ishida, M. Nagaoka, T. Akita, M. Haruta, Chem. Eur. J. 14 (2008) 8456.
[12] J. Sun, D. Ma, H. Zhang, X. Liu, X. Han, X. Bao, G. Weinberg, N. Pfander, D. Su, J. Am. Chem. Soc. 128 (2006) 15756.
[13] C. Yang, H. Shen, K. Chao, Adv. Funct. Mater. 12 (2002) 143.
[14] L. Li, J.L. Shi, L.X. Zhang, L.M. Xiong, J.N. Yan, Adv. Mater. 16 (2004) 1079.
[15] C. Wang, G. Zhu, J. Li, X. Cai, Y. Wei, D. Zhang, S. Qiu, Chem. Eur. J. 11 (2005) 4975.
[16] M.P. Mokhonoana, N.J. Coville, A.K. Datye, Catal. Lett. 135 (2010) 1.
[17] H. Lee, S.E. Habas, S. Kweskin, D. Butcher, G.A. Somorjai, P. Yang, Angew. Chem. Int. Ed. 45 (2006) 7824.
[18] T.K. Sau, C.J. Murphy, J. Am. Chem. Soc. 126 (2004) 8648.
[19] H. Wang, S. Deng, Z. Shen, J. Wang, D. Ding, T. Chen, Green Chem. 11 (2009) 1499.
[20] L. Martins, W. Holderich, P. Hammer, D. Cardoso, J. Catal. 271 (2010) 220.
[21] Y. Kubota, H. Ikeya, Y. Sugi, T. Yamada, T. Tatsumi, J. Mol. Catal. A: Chem. 249 (2006) 181.
[22] Y. Kubota, Y. Nishizaki, H. Ikeya, M. Saeki, T. Hida, S. Kawazu, M. Yoshida, H. Fujii, Y. Sugi, Micropor. Mesopor. Mater. 70 (2004) 135.
[23] A.C. Oliveira, L. Martins, D. Cardoso, Micropor. Mesopor. Mater. 120 (2009) 206.
[24] L. Martins, D. Cardoso, Micropor. Mesopor. Mater. 106 (2007) 8.
[25] L. Martins, T.J. Bonagamba, E.R. Azevedo, P. Bargiela, D. Cardoso, Appl. Catal. A: Gen. 312 (2006) 77.
[26] T. Jiang, Q. Zhao, M. Li, H. Yin, J. Hazar. Mater. 159 (2008) 204.
[27] A. Bhaumik, S. Inagaki, J. Am. Chem. Soc. 123 (2001) 691.
[28] A.H. Lu, W.C. Li, Z. Hou, F. Schuth, Chem. Commun. (2007) 1038.
[29] A.K. Prashar, R.P. Hodgkins, J.N. Chandran, P.R. Rajamohanan, R.N. Devi, Chem. Mater. 22 (2010) 1633.
[30] R. Xing, Y. Liu, H. Wu, X. Li, M. He, P. Wu, Chem. Commun. (2008) 6297.
[31] B. Karimi, A. Zamani, S. Abedi, J.H. Clark, Green Chem. 11 (2009) 109.
[32] T. Mallat, A. Baiker, Chem. Rev. 104 (2004) 3037.
[33] K. Mori, K. Yamaguchi, T. Hara, T. Mizugaki, K. Ebitani, K. Kaneda, J. Am. Chem. Soc. 124 (2002) 11572.
[34] K. Mori, T. Hara, T. Mizugaki, K. Ebitani, K. Kaneda, J. Am. Chem. Soc. 126 (2004) 10657.
[35] D.I. Enache, J.K. Edwards, P. Landon, B.S. Espriu, A.F. Carley, A.A. Herzing, M. Watanabe, C.J. Kiely, D.W. Knight, G.J. Hutching, Science 311 (2006) 362.
[36] N. Dimitratos, J.A. Lopez-Sanchez, D. Morgan, A.F. Carley, R. Tiruvalam, C.J. Kiely, D. Bethell, G.J. Hutchings, Phys. Chem. Chem. Phys. 11 (2009) 5142.
[37] N. Dimitratos, A. Villa, D. Wang, F. Porta, D. Su, L. Prati, J. Catal. 244 (2010) 113.

[38] A. Villa, N. Janjic, P. Spontoni, D. Wang, D. Su, L. Prati, Appl. Catal. A 364 (2009) 221.
[39] A. Abad, P. Concepcion, A. Corma, H. Garcia, Angew. Chem. Int. Ed. 44 (2005) 4066.
[40] A. Abad, C. Almela, A. Corma, H. Garcia, Chem. Commum. (2006) 3178.
[41] A. Abad, A. Corma, H. Garcia, Chem. Eur. J. 14 (2008) 212.
[42] Y. Liu, H. Tsunoyama, T. Akita, T. Tsukuda, Chem. Commun. 46 (2010) 550.
[43] Y. Zhu, H. Qian, M. Zhu, R. Jin, Adv. Mater. 22 (2010) 1915.
[44] N.S. Patil, B.S. Uphade, P. Jana, S.K. Bharagava, V.R. Choudhary, J. Catal. 223 (2004) 236.
[45] J. Huang, T. Takei, T. Akita, H. Ohashi, M. Haruta, Appl. Catal. B 95 (2010) 430.
[46] T. Liu, P. Hacarlioglu, S.T. Oyama, M.F. Luo, X.R. Pan, J.Q. Lu, J. Catal. 267 (2009) 202.